



**Signature of tropical  
fires in the diurnal  
cycle of tropospheric  
CO as seen from  
Metop-A/IASI**

T. Thonat et al.

# Signature of tropical fires in the diurnal cycle of tropospheric CO as seen from Metop-A/IASI

**T. Thonat, C. Crevoisier, N. A. Scott, A. Chédin, R. Armante, and L. Crépeau**

Laboratoire de Météorologie Dynamique, CNRS, IPSL, Ecole Polytechnique, Palaiseau, France

Received: 23 July 2014 – Accepted: 17 September 2014 – Published: 17 October 2014

Correspondence to: T. Thonat (thibaud.thonat@lmd.polytechnique.fr)

Published by Copernicus Publications on behalf of the European Geosciences Union.

Title Page

Abstract

Introduction

Conclusions

References

Tables

Figures

◀

▶

◀

▶

Back

Close

Full Screen / Esc

Printer-friendly Version

Interactive Discussion



## Abstract

Five years (July 2007–June 2012) of CO tropospheric columns derived from the IASI hyperspectral infrared sounder onboard Metop-A are used to study the impact of fires on the concentrations of CO in the mid-troposphere. Following Chédin et al. (2005, 2008), who showed the existence of a daily tropospheric excess of CO<sub>2</sub> quantitatively related to fire emissions, we show that tropospheric CO also displays a diurnal signal with a seasonality that is in very good agreement with the seasonal evolution of fires given by GFED3.1 (Global Fire Emission Database) emissions and MODIS (Moderate Resolution Imaging Spectroradiometer) burned area. Unlike daytime or nighttime CO fields, which mix local emissions with nearby emissions transported to the region of study, the day-night difference of CO allows to highlight the CO signal due to local fire emissions. A linear relationship is found in the whole tropical region between CO fire emissions from the GFED3.1 inventory and the diurnal difference of IASI CO ( $R^2 \sim 0.6$ ). Based on the specificity of the two main phases of the combustion (flaming vs. smoldering) and on the vertical sensitivity of the sounder to CO, the following mechanism is proposed to explain such a CO diurnal signal: at night, after the passing of IASI at 9.30 p.m. LT, a large amount of CO emissions from the smoldering phase is trapped in the boundary layer before being uplifted the next morning by natural and pyro-convection up to the free troposphere, where it is seen by IASI at 9.30 a.m. LT. The results presented here highlight the need for developing complementary approaches to bottom-up emissions inventories and for taking into account the specificity of both the flaming and smoldering phases of fire emissions in order to fully take advantage of CO observations.

## 1 Introduction

By combining human and natural components, biomass burning plays an important and singular role in the global carbon cycle. Fire emissions are indeed a major source

ACPD

14, 26003–26039, 2014

### Signature of tropical fires in the diurnal cycle of tropospheric CO as seen from Metop-A/IASI

T. Thonat et al.

Title Page

Abstract

Introduction

Conclusions

References

Tables

Figures

◀

▶

◀

▶

Back

Close

Full Screen / Esc

Printer-friendly Version

Interactive Discussion



of carbon in the atmosphere, particularly in the forms of carbon dioxide (CO<sub>2</sub>) and carbon monoxide (CO). According to van der Werf et al. (2010), the mean global emission in the 1997–2009 period is up to 2.0 Pg C yr<sup>-1</sup>. This represents the equivalent of about one third of the total anthropogenic emissions related to fossil fuel combustion and cement production (IPCC, 2007). These global emissions are not in total a net contribution to the atmosphere since the carbon released is partly recaptured by photosynthesis during the consecutive growth of plants. Nonetheless, they are important enough to be the main factor driving the variability of the CO<sub>2</sub> growth rate (Lagenfelds et al., 2002). The influence of fires on climate occurs in several ways: they have an impact on the components of radiative forcing and globally reinforce climate change (Bowman et al., 2009); they globally reduce surface albedo by producing soot; they release various chemical compounds which can reach the free troposphere (Lavoué, 2000) and then be transported around the globe (e.g., Freitas et al., 2006; Guan et al., 2008) and affect the atmospheric chemistry; aerosols emitted by fires can modify cloud coverage and precipitation patterns. However, despite their magnitude, current estimates of fire emissions of gases and aerosols still remain affected by large uncertainties.

Throughout the years, several fire emission inventories have been built based on various approaches (e.g., Hoelzemann et al., 2004; Jain et al., 2006; Lehsten et al., 2009; van der Werf et al., 2010). Most of them rely on the following equation to compute fire emissions:

$$M = A \cdot B \cdot e \cdot EF \quad (1)$$

where  $M$  (g) is the product of the burned areas  $A$  (m<sup>2</sup>), the biomass density  $B$  (g m<sup>-2</sup>), the combustion efficiency  $e$  (g g<sup>-1</sup>) and the emission factor  $EF$  which depends on the studied gas (Seiler and Crutzen, 1980).  $A$  is generally determined from observations from space,  $B$  and  $e$  are given by a biogeochemical model and  $EF$  is calculated empirically. However, large uncertainties affect each term of this equation, meaning that these inventories alone are not sufficient to determine all the characteristics of fires and their emissions.

## Signature of tropical fires in the diurnal cycle of tropospheric CO as seen from Metop-A/IASI

T. Thonat et al.

Title Page

Abstract

Introduction

Conclusions

References

Tables

Figures

◀

▶

◀

▶

Back

Close

Full Screen / Esc

Printer-friendly Version

Interactive Discussion



A more direct measure from space, which is by nature global and continuous, of biomass burning carbon emissions themselves, and more particularly of CO<sub>2</sub> and CO, could in principle allow to avoid these difficulties and provide an indispensable complement to the inventories. Several studies have relied on CO observation from space, mostly from thermal infrared sounders, to quantify fire emissions. Indeed, since fires emit large amount of CO in the atmosphere far above its background level, CO is known as a good proxy of fire emissions. For example, continuous CO measurements, in particular with the MOPITT (Measurements of Pollution in the Troposphere) instrument, have been compared to chemistry-transport simulations based on fire emission inventories (e.g., Turquety et al., 2007; Yurganov et al., 2008). AIRS (Atmospheric Infrared Sounder) was the first instrument to provide daily global measurements of CO, highlighting the large-scale transport of fire emissions (McMillan et al., 2005, 2008). Observations from the more recent IASI (Infrared Atmospheric Sounding Interferometer) instrument (Hilton et al., 2012) have also been used, for example to retrieve CO fire emissions in Greece in 2007, showing their undervaluation in the GFED2 (Global Fire Emission Database) inventory (Turquety et al., 2009), or to study extreme fire events in Russia in 2010 (Yurganov et al., 2011). CO is a good indicator of fire activity, but it only represents a small fraction of the emissions, which is mostly representative of the smoldering phase of the combustion (Lobert and Warnatz, 1993). Therefore CO<sub>2</sub>, which represents the majority of the emissions, mostly representative of the flaming phase of the combustion, has also been studied in relation with fire activity, despite the difficulty of both retrieving CO<sub>2</sub> from space and capturing the “fire signal” in its tropospheric concentration.

A new approach developed by Chedin et al. (2005, 2008) allows to isolate CO<sub>2</sub> fire emissions from space, by calculating the difference between CO<sub>2</sub> retrieved by night and CO<sub>2</sub> retrieved by day that results from the diurnal cycle of fires (Giglio, 2007). This difference is calculated from the observations of TOVS (TIROS-N Operational Vertical Sounder) onboard NOAA10 and is called Daily Tropospheric Excess (DTE). It can reach several ppmv (parts per million by volume) over regions affected by fires.

# Signature of tropical fires in the diurnal cycle of tropospheric CO as seen from Metop-A/IASI

T. Thonat et al.

Title Page

Abstract

Introduction

Conclusions

References

Tables

Figures

◀

▶

◀

▶

Back

Close

Full Screen / Esc

Printer-friendly Version

Interactive Discussion



# Signature of tropical fires in the diurnal cycle of tropospheric CO as seen from Metop-A/IASI

T. Thonat et al.

Title Page

Abstract

Introduction

Conclusions

References

Tables

Figures

◀

▶

◀

▶

Back

Close

Full Screen / Esc

Printer-friendly Version

Interactive Discussion



The seasonal and interannual variabilities of the DTE are in agreement with the ones of burned areas and fire emissions, showing that there is an excess of CO<sub>2</sub> in the troposphere above burned areas at 7.30 p.m., few hours after the peak of fire activity, compared to the CO<sub>2</sub> level at 7.30 a.m. The DTE was shown to be quantitatively related to CO<sub>2</sub> fire emissions in the tropics. The mechanism explaining the observation of such a signal is as follows: (i) in the afternoon, during the period of high fire activity, large quantities of CO<sub>2</sub> are emitted into the free troposphere, (ii) CO<sub>2</sub> accumulates under the tropopause and is seen by the satellite at 7.30 p.m., (iii) CO<sub>2</sub> is then diluted by large-scale transport during the 12 h preceding the next pass of the satellite, at 7.30 a.m., before fires start again. Rio et al. (2010) confirmed theoretically this result with a pyrothermal plume model.

As Metop passing times are 9.30 a.m./p.m., i.e. before and after the maximum of the diurnal cycle of fires, IASI is well suited to complete the study of the diurnal cycle of fire emissions initiated with TOVS. The main difficulty of the DTE remains in the retrieval of CO<sub>2</sub> and the weakness of the CO<sub>2</sub> fire signal. On the contrary, the impact of fires on the concentration of CO can be more than 100 % of its background level (e.g., Turquety et al., 2009), making it easier to measure. For these reasons, our study focuses on CO, and particularly on its diurnal variation in relation to fire activity. Our study focuses on the tropics, where the majority of fire emissions are located, during the 5 years between 2007 and 2012. Section 2 describes the data and the method used to retrieve CO from the IASI observations. Section 3 presents the IASI retrievals, by day and by night, in comparison with fire activity. We first focus on southern Africa, where fire emissions are particularly strong, and then on the whole tropical region. Section 4 is a discussion on why the diurnal difference of CO is in better agreement with fire activity than the daytime or nighttime concentrations. Section 5 concludes this study.

## 2 Data and method

### 2.1 IASI

The Infrared Atmospheric Sounding Interferometer (IASI) is a polar-orbiting nadir-viewing instrument that measures infrared radiation emitted from the Earth. IASI is a high resolution Fourier Transform Spectrometer based on a Michelson Interferometer, which provides 8461 spectral samples, ranging from 645 to 2760  $\text{cm}^{-1}$  (15.5 and 3.6  $\mu\text{m}$ ), with a spectral sampling of 0.25  $\text{cm}^{-1}$ , and a spectral resolution of 0.5  $\text{cm}^{-1}$  after apodisation (“Level 1c” spectra). IASI cross track scanning is of 2200 km, allowing global coverage twice a day. The instantaneous field of view is sampled by  $2 \times 2$  circular pixels whose ground resolution is 12 km at nadir. IASI was developed by the Centre National d’Etudes Spatiales (CNES) in collaboration with the European Organisation for the Exploitation of Meteorological Satellites (EUMETSAT); it was launched in October 2006 onboard the polar-orbiting Meteorological Operational Platform (Metop-A), and is operational since July 2007. In this study, use is made of the Level 1c data (available from the Ether Centre for Atmospheric Chemistry Products and Services website: <http://ether.ipsl.jussieu.fr/>, via EUMETCAST).

### 2.2 Retrieval method

The retrieval scheme is based on the double difference approach described in Thonat et al. (2012), which takes advantage of the high spectral resolution of IASI. It relies on the idea of using a difference in brightness temperature (BT) between two channels having the same sensitivities to every atmospheric and surface variable but CO. This difference is thus only sensitive to CO variations and cancels out the signals coming from interfering variables (surface temperature and emissivity, temperature, water vapour and nitrous oxide). In order to interpret this BT difference in terms of CO, we use the difference between the BT simulated by the 4A (Automatized Atmospheric Absorption Atlas) (Scott and Chédin, 1981; <http://ara.abct.lmd.polytechnique.fr/>) radiative

ACPD

14, 26003–26039, 2014

**Signature of tropical fires in the diurnal cycle of tropospheric CO as seen from Metop-A/IASI**

T. Thonat et al.

Title Page

Abstract

Introduction

Conclusions

References

Tables

Figures

◀

▶

◀

▶

Back

Close

Full Screen / Esc

Printer-friendly Version

Interactive Discussion



transfer model and the observed BT. The double difference then provides the amount of CO in the troposphere which is in excess (or deficit) in comparison with the a priori CO profile used as input in 4A.

For the simulated BT, use is made of ECMWF ERA-INTERIM Reanalyses as atmospheric data input to 4A. These are profiles of temperature, water vapour and ozone characterized by a 6 h time resolution and a  $0.75^\circ \times 0.75^\circ$  space resolution, colocalised in time and space to IASI clear-sky fields of view and inter/extrapolated on the 4A pressure levels. The surface temperature is estimated directly from one IASI channel (at  $2501.75 \text{ cm}^{-1}$ ) to avoid the lag between the closest reanalyses and the IASI passing. The same a priori CO profile is used for every simulation. For observed BT, clouds and aerosols are detected with several threshold tests based on IASI and AMSU observations (Crevoisier et al., 2003; Pierangelo et al., 2004).

The retrieved CO column is representative of the mid-troposphere, with a maximum sensitivity at about 450 hPa, depending on the difference between surface temperature and above air temperature: the higher this difference, the higher the sensitivity to CO in the lower layers of the troposphere. A negative thermal contrast has symmetric effects. The retrieval method also gives access to the precision, which is about 2.5 ppbv.

CO retrievals from IASI have been compared with the CARIBIC (Civil Aircraft for the Regular Investigation of the Atmosphere Based on an Instrument Container) (Breninkmeijer et al., 2007) aircraft measurements. The difference between CARIBIC and IASI CO is on average 3.6 ppbv, with a SD of 13.0 ppbv. This good agreement is also found above deserts and mountainous areas, highlighting that the retrievals are not impacted by surface characteristics (Thonat et al., 2012).

## Signature of tropical fires in the diurnal cycle of tropospheric CO as seen from Metop-A/IASI

T. Thonat et al.

[Title Page](#)[Abstract](#)[Introduction](#)[Conclusions](#)[References](#)[Tables](#)[Figures](#)[◀](#)[▶](#)[◀](#)[▶](#)[Back](#)[Close](#)[Full Screen / Esc](#)[Printer-friendly Version](#)[Interactive Discussion](#)

### 3 The diurnal variation of mid-tropospheric CO

#### 3.1 IASI daytime and nighttime CO over the tropics

Five whole years of clear-sky observations from the IASI hyperspectral infrared sounder between July 2007 and June 2012 have been interpreted in terms of mid-tropospheric CO column, in the tropics (30°S, 30°N), by day and night (9.30 a.m./p.m. LT). Maps of monthly means of CO in the troposphere are plotted in Fig. 1 for January, April, July and October 2008, over land and over sea. Blank areas denote an absence of retrievals due to persistent cloudiness or aerosols. According to Fig. 1, the distribution and the seasonality of CO retrieved by day and by night are the same, though with lower maximum values in the nighttime.

Extreme CO concentrations (superior to ~ 110 ppbv) are localised above continents, in the Northern Hemisphere (NH) during the boreal winter and in the Southern Hemisphere (SH) during the austral winter. These extreme values, that concern primarily Africa and South America, stem from important biomass burnings events in the local dry season (Duncan et al., 2003). Fires are not the only source of CO in the tropics; for example high CO values are seen in China outside of the fire season, caused by a continuous pollution coming from fossil fuel combustion (industry, transport) (Buchwitz et al., 2007; Streets et al., 2006).

The repartition of CO seen in Fig. 1 is also influenced by the seasonal variation of the OH radical, the main sink of CO (Holloway, 2000). During the boreal winter, OH concentrations are low in the North and high in the South (Spivakovsky et al., 1990), allowing CO emitted by fires and human activities to accumulate in the NH (Duncan et al., 2007). The opposite happens during the winter in the SH, where the anthropogenic emissions play a less important role.

High CO concentrations are also seen over sea because of the transport from continental sources. Indeed, in the mid-troposphere, where IASI retrievals are most sensitive to CO (~ 450 hPa), stronger winds and a longer lifetime of CO than at the surface make the transport of CO over long distances possible.

### Signature of tropical fires in the diurnal cycle of tropospheric CO as seen from Metop-A/IASI

T. Thonat et al.

Title Page

Abstract

Introduction

Conclusions

References

Tables

Figures

◀

▶

◀

▶

Back

Close

Full Screen / Esc

Printer-friendly Version

Interactive Discussion





Even if the signature of fire emissions on tropospheric CO fields is well seen, the existence of other sources than fires and the transport of fire emissions by atmospheric circulation make the study of the relation between fires and CO concentrations difficult. In order to enhance the links between fire activity and tropospheric CO, we now take advantage of the availability provided by infrared sounders to retrieve CO both by day and night.

## 3.2 A case study: diurnal variation of CO over southern Africa

### 3.2.1 IASI daytime and nighttime CO

We now focus our study in southern Africa (between 20° S and 0° in latitudes, and 0° and 53° E in longitudes) since biomass burning is particularly strong in this region. Moreover, as opposed to northern Africa, southern Africa is rather preserved from strong pollution and dust events (Engelstaedter et al., 2006).

Figure 2a and b shows the monthly means of the integrated content of CO from IASI between January and December 2008, by day (9.30 a.m.) and night (9.30 p.m.). The same spatio-temporal distribution of CO is seen on both time series. However, values of IASI CO by day are stronger than the ones by night. During the dry season, there is an excess of CO shifting progressively from the North-West in May to the South and South-East until November. This excess of tropospheric CO reaches a maximum in September–October. This evolution can be explained by the evolution of fires (Cahoon et al., 1992; Barbosa et al., 1999); it is similar to the evolution of the burned areas (BA) observed by MODIS (Moderate Resolution Imaging Spectroradiometer) (Roy et al., 2008) (Fig. 2c), but with a shift of two months. In addition, the excesses of CO in the troposphere are not located exactly above the burned areas, highlighting the transport of the CO emitted by fires, by convection and general atmospheric circulation.

The 2 months lag between the day/night retrieved CO and fires is observed for each of the 5 years studied here, as shown in Fig. 3, which represents the evolution of the monthly means of IASI CO by day and night, MODIS BA and CO emissions from

## Signature of tropical fires in the diurnal cycle of tropospheric CO as seen from Metop-A/IASI

T. Thonat et al.

Title Page

Abstract

Introduction

Conclusions

References

Tables

Figures

◀

▶

◀

▶

Back

Close

Full Screen / Esc

Printer-friendly Version

Interactive Discussion



GFED3.1, in the same region as Fig. 2. It is worth noting that there are also disagreements between MODIS BA and GFED3.1 emissions concerning the evolution of fires during the dry season. For example, according to GFED3.1, the maximum of the emissions generally occurs a month after the maximum of the burned areas. These discrepancies are due to the fact that the emissions are not proportional to the burned areas and that many other variables are taken into account in their calculation, like the type of vegetation, the combustion efficiency or the emission factor.

In April, which is a month of transition between the dry season in the North and the dry season in the South, IASI CO is minimum; it starts to increase in May, at the beginning of the fire season. In September–October, the maximum of the CO mixing ratio in the troposphere corresponds to the maximum of the GFED fire emissions in 2008 and 2011 but is one to two months delayed in the other years. In November, although fires are hardly active according to the MODIS BA and GFED3.1, values of CO are still quite high.

Between December and February, i.e. outside of the fire season in the SH, CO values are in general still quite high between 0 and 5° S. This is due to the southward transport of CO emitted by northern fires and pollution. Such atmospheric processes complicate the analysis of the CO fields retrieved from space observations and our ability to disentangle the CO directly emitted by fire over the region of interest from the background and transported CO from nearby regions. This is why, following Chédin et al. (2005), we now focus on the analysis of the day-night difference of CO.

### 3.2.2 Day-night difference of IASI CO

Monthly means of day-night differences of CO are plotted in Fig. 2d. The day-night difference is calculated out of the  $0.75^\circ \times 0.75^\circ$  means of the clear-sky retrievals of CO made at 9.30 a.m. and 9.30 p.m. on the exact same day, and then averaged over the whole month. Blank areas on the maps of Fig. 2d are due to a lack of points caused by the presence of clouds or aerosols, or by the fact that the daytime and the nighttime orbits of the sounder do not overlap over these areas. The 5 years evolution of the

monthly means of the day-night differences of CO in southern Africa, along with the evolution of MODIS BA and GFED3.1 emissions, are plotted in Fig. 4.

Unlike the evolution of daytime and nighttime CO (Fig. 3), the evolution of the diurnal difference is in very good agreement with fire activity. The maps of the diurnal difference show a positive signal between May and October which can exceed 40 ppbv. The day-night signal is observed just above fires, and follows their evolution between May and September, shifting towards South and South-East, with a maximum in September, at the same time as for the emissions, or one month later. Between November and April, i.e. outside of the fire season, although the values of CO retrieved either by day or by night are quite high because of the transport from the NH, the day-night difference of CO is almost null. Over sea, the day-night difference is null. This shows that the chosen differential approach emphasizes the CO emitted by fires while cancelling out the background CO stemming from CO emitted in other regions and then transported over the region of interest.

Despite this good agreement between IASI diurnal CO (Fig. 2d) and fire activity given by GFED3.1 emissions and MODIS burned areas (Fig. 2c), some discrepancies can be found between the two of them. For instance, between July and September, the day-night difference of IASI CO between 35° E and 40° E is low despite high level of burned areas seen by MODIS. In addition, in October, the diurnal difference is very high even though fires are very weak. The decrease of the signal takes place a little bit later than the one of fires; the signal is still important in November in 2010 and 2011 albeit fires are not active any more according to MODIS and GFED3.1 (Fig. 4). This kind of discrepancy in seasonality with an emission inventory has already been observed for this area with GFED2 (Edwards et al., 2006; van der Werf et al., 2006; Roberts et al., 2009). This lag could be due to the burning of woody fuels towards the end of the dry season, that may not be well represented in the inventory. These dense fuels emit large amounts of CO and are likely to burn on a long period. After the peak of the fire season, the smoldering phase of the combustion, which is characterized by thermodynamical conditions of higher moisture and lower temperature, favours CO

## Signature of tropical fires in the diurnal cycle of tropospheric CO as seen from Metop-A/IASI

T. Thonat et al.

Title Page

Abstract

Introduction

Conclusions

References

Tables

Figures

◀

▶

◀

▶

Back

Close

Full Screen / Esc

Printer-friendly Version

Interactive Discussion

emissions (Lobert and Warnatz, 1993) in fires that may not be captured from space because of their small energy.

### 3.2.3 Relation between the day-night difference of CO and fire emissions

14, 26003–26039, 2014

T. Thonats et al.

## Abstract

## Introduction

## Conclusions

## References

## Tables

## Figures

[Back](#)

Close

Full Screen / Esc

[Printer-friendly Version](#)

## Interactive Discussion



To study in more details the diurnal cycle of CO in southern Africa and its relation with fires, we focus on several areas represented in Fig. 5a, whose coordinates are given in Table 1. These areas, adapted from Hoelzemann (2006), correspond to different kinds of vegetation, which are represented in Fig. 5b, adapted from Mayaux et al. (2003). The dominant types in southern Africa are forests, savannas and croplands. On these areas, we calculate the mean of the day-night difference of the integrated content of CO from IASI, whose evolution is represented in Fig. 6, on average between 2008 and 2011. Also plotted are the MODIS BA and the GFED3.1 emissions for the same period.

Areas H1 and H2, in the North of the region, display the worst agreement: the background level of the diurnal signal is quite high and there is a shift of one month of the seasonality compared to fires. But these areas only have a few points available to calculate the day-night difference of CO, as explained above, and as seen in Fig. 2d.

To conclude, the agreement between fire activity and the diurnal cycle of CO in southern Africa shown in Fig. 4 is the result of an agreement between these signals at finer scales, corresponding to different kinds of vegetation. This agreement concerns the seasonality of the signals as well as their intensity, even though discrepancies arise in some areas, which can be related to the specificity of CO emissions according to the kind of vegetation, and to the lack of observations available to compute a significant day-night difference of CO.

### 3.3 Link between day-night CO and fire emissions in the whole tropical region

We now extend our study to the whole tropical zone, which is divided into 12 areas plotted in Fig. 7 and defined in Table 2. These areas are taken from Chédin et al. (2008) and are representative of the different fire seasons. Figure 8 compares the annual means of the day-night difference of CO (in ppbv) with the annual means of the GFED3.1 emissions (in  $\text{g CO m}^{-2}$ ), averaged over 2008–2011. The GFED3.1 emissions are arbitrarily multiplied by a constant factor (found to be equals to 16) in order to “reconcile” the units. Figure 8 can be compared to Fig. 11 from Chédin et al. (2008) that shows the annual GFED2 CO<sub>2</sub> emissions as a function of the DTE of CO<sub>2</sub> computed from the TOVS observations.

A linear relationship can be seen between the two variables over a large interval, between 2 and 12 ppbv. This relationship supports the interpretation of the day-night difference of CO as a signal directly related to biomass burning emissions. Two areas set apart: South-East Africa (AfSE), with a low diurnal signal, and Central America (AmC), with a high diurnal signal, compared to the emissions. Except these two areas, the correlation is high between the diurnal signal of CO and the GFED3.1 emissions

( $R^2 \sim 0.6$ ); however it is lower than the correlation between the DTE of  $\text{CO}_2$  and the emissions found by Chédin et al. (2008) ( $R^2 \sim 0.8$ ).

As stressed by Chédin et al. (2008) for  $\text{CO}_2$ , the discrepancies between the emissions and the diurnal signal in the troposphere can be related to the atmospheric transport of the emissions or to complex diurnal cycles of the emissions. They also may come from a mischaracterisation of the specificity of CO emissions, especially from the smoldering fire phase, in GFED3.1. In particular, most of GFED3.1 emission factors are based on averages per biome that do not take into account spatial variability, although they are influenced by several environmental factors.

## 4 Discussion

### 4.1 Impact of the vertical sensitivity of the sounder on the day-night difference of CO

As seen in Fig. 4 (or Fig. 6), the diurnal excess of CO is still positive outside of the fire season, even if it stays low. Given that there is no other significant diurnal source of CO in southern Africa, these signals can be explained by the diurnal variation of the vertical sensitivity of the CO retrieval. As seen in Fig. 9, which represents the IASI CO weighting functions in southern Africa, the weighting functions during daytime display a higher sensitivity to CO close to the surface, due to a higher thermal contrast (i.e. the difference between the surface temperature and the temperature of the first pressure level), during and outside of the fire season (July and January, respectively) (Thonat et al., 2012).

As was explained in Sect. 2.2, the retrieved tropospheric column of CO  $q\text{CO}$  is the sum of the integrated content of the input profile of the radiative transfer model 4A and of the excess (or deficit) of CO estimated in respect to it. This means:

$$q\text{CO} = q\text{CO}^{4A} + \Delta q\text{CO} \quad (2)$$

The first term of this sum is given by:

$$qCO^{4A} = \sum_{i=1}^{42} wp_i \cdot profileCO_i^{4A} \quad (3)$$

where  $i$  is the number of the pressure layer,  $wp$  is the weighting function of CO for the given retrieval (in ppbv ppbv<sup>-1</sup>) and  $profileCO^{4A}$  is the profile used as input in 4A for every simulation.

Figure 10 shows the evolution of the day-night difference of  $qCO^{4A}$ , on the same period and on the same area as in Fig. 4. Given that only one profile is used as input in 4A, the diurnal signal in Fig. 10 is only due to the diurnal variations of the weighting function. Naturally, the second term of the sum in Eq. (2),  $\Delta qCO$ , is also dependent on the weighting function. But quantifying the impact of the diurnal variations of the weighting function on this term (thus on  $qCO$ ) would require to know the “true” profiles of CO corresponding to the passes of the sounder, whether these profiles come from observations or simulations of a chemistry-transport model. That’s why here we only focus on the day-night difference of  $qCO^{4A}$ , which gives an approximation of the influence of the weighting functions, and which can be compared to the diurnal signal of CO in Fig. 4.

As expected, the signal is positive and has almost the same seasonality as the diurnal signal shown in Fig. 4, with a shift of one month. It is about 5 ppbv between December and April, which coarsely corresponds to the bias observed in Fig. 4 for these months, April excepted. This result can suggest that the diurnal excess of CO observed when there is no fire just comes from the diurnal variations of the weighting function. In addition, the amplitude of the signal in Fig. 10 is only about 2 ppbv whereas it is 15 ppbv in Fig. 4.

This first approximation of the impact of the variation of the vertical sensitivity on the day-night difference of CO suggests that the diurnal tropospheric excess of CO retrieved from IASI is mostly due to the diurnal cycle of fire emissions.

## Signature of tropical fires in the diurnal cycle of tropospheric CO as seen from Metop-A/IASI

T. Thonat et al.

Title Page

Abstract

Introduction

Conclusions

References

Tables

Figures

◀

▶

◀

▶

Back

Close

Full Screen / Esc

Printer-friendly Version

Interactive Discussion





4.2 Hypothesis on the mechanisms explaining the relation between fires and the day-night difference of CO

As exposed in Sect. 3.3, the diurnal signals of CO and CO<sub>2</sub> are of opposite signs: CO<sub>2</sub> concentrations in the troposphere are higher by night, whereas the CO concentrations are higher in the daytime. Several factors can explain this sign difference.

As said above, CO and CO<sub>2</sub> are emitted during the flaming and the smoldering phases of the combustion, in which their emissions are anti-correlated. The flaming phase favours CO<sub>2</sub> emissions (Lobert and Warnatz, 1993); it is characterized by high temperatures (800–1200 °C) (Pyne et al., 1996) which entail strong uprisings, and is associated with the combustion of the aboveground biomass. So, during the day, in this phase, fires emit large quantities of CO<sub>2</sub> reaching the high troposphere. At the end of the day, the infrared sounder's measurements, which are representative of the high troposphere, allow to observe this accumulation of fire emissions under the tropopause. Conversely, at the beginning of the day, after the emissions have been diluted and before fires start again (or: before the emissions can reach such altitudes), the sounder only observes the background level of CO<sub>2</sub> (Chédin et al., 2005, 2008).

The other phase of the combustion, the smoldering phase, favours CO emissions (Lobert and Warnatz, 1993); it is characterized by lower temperatures (100–600 °C) (Pyne et al., 1996), which contribute to more stable plumes, more prone to be driven by the variability of the boundary layer; it is associated with the combustion of the organic layer. At the end of the day, still active fires lose their efficiency, favouring CO emissions in the smoldering phase (Ward et al., 1996; Kasischke and Bruhwiler, 2003).

The fact that the smoldering phase can last long, with CO plumes staying close to the surface, entails high CO concentrations in the first layers, in particular at night. For example, Ferguson et al. (2003) measured in Alaska extreme CO concentrations at midnight, reaching 27 ppmv, between 0 and 150 m altitude. These extreme concentrations are the consequence of a very stable boundary layer. Ferguson et al. (2003)

Signature of tropical fires in the diurnal cycle of tropospheric CO as seen from Metop-A/IASI

T. Thonat et al.

Title Page

Abstract

Introduction

Conclusions

References

Tables

Figures

◀

▶

◀

▶

Back

Close

Full Screen / Esc

Printer-friendly Version

Interactive Discussion





## Signature of tropical fires in the diurnal cycle of tropospheric CO as seen from Metop-A/IASI

T. Thonat et al.

Title Page

Abstract

Introduction

Conclusions

References

Tables

Figures

◀

▶

◀

▶

Back

Close

Full Screen / Esc

Printer-friendly Version

Interactive Discussion



observed almost no smoke at about 2000 m. The day after, fires are less active, and the concentrations are much lower, of the order of a ppmv. The extreme concentrations of the previous day were dissipated by the natural convection and advection. Even though this is an example of a boreal forest fire, it highlights the possibility that, while fires can be very active during the day, with emissions reaching the free troposphere, the majority of the smoke is trapped at very low altitudes at night, and then uplifted in the morning by the natural convection and the pyroconvection.

Figure 11 shows the mean boundary layer height in southern Africa, in July 2008, i.e. during the fire season, calculated from the ECMWF forecasts. The boundary layer is very low, at about 200 m., between 6.00 p.m. and 3.00 a.m. The natural convection is becoming important only after 6.00 a.m. When IASI passes at 9.30 p.m., CO emissions happening at night are trapped in the boundary layer, so they are not visible by the sounder, which is sensitive to CO in the mid-troposphere and insensitive to CO close to the surface by night, as shown in Fig. 9. When IASI passes at 9.30 a.m., the trapped CO has been uplifted by natural convection and reaches altitudes to which the sounder is sensitive to CO. In addition, at 9.30 a.m., fires are active again (mostly in the flaming phase of the combustion), with strong vertical movements that can uplift surrounding smokes. As a result, above burning areas, the day-night difference of CO computed from IASI is a positive signal directly related to fire emissions.

These different factors support the hypothesis of the convection of CO emissions in the mid-troposphere in the morning, following their accumulation in the boundary layer during the night. The sign difference between the diurnal signals of CO and CO<sub>2</sub> is the result of the specificity of the two phases of the combustion and of the difference in the sounder's vertical sensitivity to these two gases.

## 5 Conclusions

The relation between tropical biomass burning emissions and CO has been analysed by interpreting 5 years (2007–2012) of mid-tropospheric CO column retrieved from IASI

observations by day and by night (9.30 a.m./p.m. LT), and temporal series of burned areas (MODIS) and fire emissions (GFED3.1). Following Chédin et al. (2005, 2008) who related the diurnal signature of CO<sub>2</sub> retrieved from NOAA10/TOVS instruments to fire emissions, we have taken advantage of the fact that IASI overpasses every point twice a day, before and after the maximum of the diurnal cycle of fires, in order to relate directly fires and CO concentrations in the troposphere.

Unlike retrievals by day or by night, the spatio-temporal evolution of the diurnal signal of tropospheric CO as retrieved from IASI, defined here as the day-night difference of CO, is in agreement with the evolution of fires: this differential approach cancels out the background CO, including plumes due to advective transport from nearby regions, and is only sensitive to the CO related to local fire emissions. A linear relationship is found in the whole tropical region between CO fire emissions from the GFED3.1 inventory and the diurnal difference of IASI CO ( $R^2 \sim 0.6$ ). For regions near the equator, daytime and nighttime orbits of the sounder overlap less, inducing a limited number of clear-sky spots available.

Some discrepancies arise between GFED emissions and IASI CO in southern Africa (i) in terms of seasonality: in regions of wooden savannas, the fire activity suggested by the IASI day-night difference of CO is more intense towards the end of the fire season (September) than GFED3.1 emissions indicate. It might be due to the fact that these regions with dense fuel are likely to favour carbon emissions during the smoldering phase up until the end of the fire season, (ii) in terms of intensity: this could indicate that the specificity of CO emissions compared to CO<sub>2</sub> emissions for each biome might need to be refined in the emission inventory's framework.

The diurnal signals of CO<sub>2</sub> from TOVS (Chédin et al., 2005, 2008) and CO from IASI are of opposite signs. CO retrievals are indeed higher in the daytime than in the nighttime, unlike CO<sub>2</sub> retrievals. The suggested mechanism explaining the diurnal signal of CO is as follows: CO is emitted in large quantities in the smoldering phase of the combustion occurring during the night (after that fires in the flaming phase have burned the above ground vegetation in the daytime), and accumulates in the boundary layer, until

## Signature of tropical fires in the diurnal cycle of tropospheric CO as seen from Metop-A/IASI

T. Thonat et al.

[Title Page](#)[Abstract](#)[Introduction](#)[Conclusions](#)[References](#)[Tables](#)[Figures](#)[◀](#)[▶](#)[◀](#)[▶](#)[Back](#)[Close](#)[Full Screen / Esc](#)[Printer-friendly Version](#)[Interactive Discussion](#)

being uplifted from the beginning of the day. This hypothesis is supported both by the specificity of CO emissions compared to CO<sub>2</sub> emissions, as well as by the fact that the retrievals of these gases are not representative of the same part of the atmosphere. Simulations with general circulation models should help to validate the plausibility of this mechanism, and to compare the effects of vertical transport patterns related to the different combustion phases on the injection of CO and CO<sub>2</sub> in the mid and upper troposphere. The results presented here show that the analysis of diurnal variations of CO and CO<sub>2</sub> as measured from space can give us a global view of the repartition of the emissions between the flaming and the smoldering phase and of their associated transport, which need to be taken into account in surface flux estimation procedures and emission inventories.

## References

- Barbosa, P. M., Stroppiana, D., Grégoire, J. M., and Pereira, J. M. C.: An assessment of vegetation fire in Africa (1981–1991): burned areas, burned biomass, and atmospheric emissions, *Global Biogeochem. Cy.*, 13, 933–950, 1999.
- Bowman, D. M. J. S., Balch, J. K., Artaxo, P., Bond, W. J., Carlson, J. M., Cochrane, M. A., D’Antonio, C. M., DeFries, R. S., Doyle, J. C., Harrison, S. P., Johnston, F. H., Keeley, J. E., Krawchuk, M. A., Kull, C. A., Marston, J. B., Moritz, M. A., Prentice, I. C., Roos, C. I., Scott, A. C., Swetnam, T. W., van der Werf, G. R., and Pyne, S. J.: Fire in Earth System, *Science*, 324, 481–484, 2009.
- Brenninkmeijer, C. A. M., Crutzen, P., Boumard, F., Dauer, T., Dix, B., Ebinghaus, R., Filippi, D., Fischer, H., Franke, H., Frieß, U., Heintzenberg, J., Helleis, F., Hermann, M., Kock, H. H., Koepfel, C., Lelieveld, J., Leuenberger, M., Martinsson, B. G., Miemczyk, S., Moret, H. P., Nguyen, H. N., Nyfeler, P., Oram, D., O’Sullivan, D., Penkett, S., Platt, U., Pupek, M., Ramonet, M., Randa, B., Reichelt, M., Rhee, T. S., Rohwer, J., Rosenfeld, K., Scharffe, D., Schlager, H., Schumann, U., Slemr, F., Sprung, D., Stock, P., Thaler, R., Valentino, F., van Velthoven, P., Waibel, A., Wandel, A., Waschitschek, K., Wiedensohler, A., Xueref-Remy, I., Zahn, A., Zech, U., and Ziereis, H.: Civil Aircraft for the regular investigation of

ACPD

14, 26003–26039, 2014

## Signature of tropical fires in the diurnal cycle of tropospheric CO as seen from Metop-A/IASI

T. Thonat et al.

Title Page

Abstract

Introduction

Conclusions

References

Tables

Figures

◀

▶

◀

▶

Back

Close

Full Screen / Esc

Printer-friendly Version

Interactive Discussion

# Signature of tropical fires in the diurnal cycle of tropospheric CO as seen from Metop-A/IASI

T. Thonat et al.

Title Page

Abstract

Introduction

Conclusions

References

Tables

Figures

◀

▶

◀

▶

Back

Close

Full Screen / Esc

Printer-friendly Version

Interactive Discussion

the atmosphere based on an instrumented container: The new CARIBIC system, Atmos. Chem. Phys., 7, 4953–4976, doi:10.5194/acp-7-4953-2007, 2007.

Buchwitz, M., Khlystova, I., Bovensmann, H., and Burrows, J. P.: Three years of global carbon monoxide from SCIAMACHY: comparison with MOPITT and first results related to the detection of enhanced CO over cities, Atmos. Chem. Phys., 7, 2399–2411, doi:10.5194/acp-7-2399-2007, 2007.

Cahoon, D. R., Stocks, B. J., Levine, J. S., Coter III, W. R., and O'Neill, C. P.: Seasonal distribution of African fires, Nature, 359, 812–815, 1992.

Chédin, A., Serrar, S., Scott, N. A., Pierangelo, C., and Ciais, P.: Impact of tropical biomass burning emission on the diurnal cycle of upper tropospheric CO<sub>2</sub> retrieved from NOAA 10 satellite observations, J. Geophys. Res., 110, D11309, doi:10.1029/2004JD005540, 2005.

Chédin, A., Scott, N. A., Armante, R., Pierangelo, C., Crevoisier, C., Foss'e, O., and Ciais, P.: A quantitative link between CO<sub>2</sub> emissions from tropical vegetation fires and the daily tropospheric excess (DTE) of CO<sub>2</sub> seen by NOAA-10 (1987–1991), J. Geophys. Res., 113, D05302, doi:10.1029/2007JD008576, 2008.

Crevoisier, C., Chédin, A., Heilliette, S., Scott, N. A., Serrar, S., Armante, R.: Mid-tropospheric CO<sub>2</sub> retrieval in the tropical zone from AIRS observations, in: Proceedings of the 13th International TOVS Study Conference, 2003.

Duncan, B. N., Martin, R. V., Staudt, A. C., Yevich, R., and Logan, J. A.: Interannual and seasonal variability of biomass burning emissions constrained by satellite observations, J. Geophys. Res., 108, 4100, doi:10.1029/2002JD002378, 2003.

Duncan, B. N., Logan, J. A., Bey, I., Megretskaia, I. A., Yantosca, R. M., Novelli, P. C., Jones, N. B., and Rinsland, C. P.: Global budget of CO, 1988–1997: source estimates and validation with a global model, J. Geophys. Res., 112, D22301, doi:10.1029/2007JD008459, 2007.

Edwards, D. P., Emmons, L. K., Gille, J. C., Chu, A., Attié, J.-L., Giglio, L., Wood, S. W., Haywood, J., Deeter, M. N., Massie, S. T., Ziskin, D. C., and Drummond, J. R.: Satellite-observed pollution from Southern Hemisphere biomass burning, J. Geophys. Res., 111, D14312, doi:10.1029/2005JD006655, 2006.

Engelstaedter, S., Tegen, I., Washington, R.: North African dust emissions and transport, Earth Sci. Rev., 79, 73–100, 2006.

# Signature of tropical fires in the diurnal cycle of tropospheric CO as seen from Metop-A/IASI

T. Thonat et al.

Title Page

Abstract

Introduction

Conclusions

References

Tables

Figures

◀

▶

◀

▶

Back

Close

Full Screen / Esc

Printer-friendly Version

Interactive Discussion



Ferguson, S. A., Collins, R. L., Ruthford, J., and Fukuda, M.: Vertical distribution of nighttime smoke following a wildland biomass fire in boreal Alaska, *J. Geophys. Res.*, 108, 4743, doi:10.1029/2002JD003324, 2003.

Freitas, S. R., Longo, K. M., and Andreae, M. O.: Impact if including the plume rise of vegetation fires in numerical simulations of associated atmospheric pollutants, *Geophys. Res. Lett.*, 33, L17808, doi:10.1029/2006GL026608, 2006.

Giglio, L.: Characterization of the tropical diurnal fire cycle using VIRS and MODIS observations, *Remote Sens. Environ.*, 108, 407–421, doi:10.1016/j.rse.2006.11.018, 2007.

Guan, H., Chatfield, R. B., Freitas, S. R., Bergstrom, R. W., and Longo, K. M.: Modeling the effect of plume-rise on the transport of carbon monoxide over Africa with NCAR CAM, *Atmos. Chem. Phys.*, 8, 6801–6812, doi:10.5194/acp-8-6801-2008, 2008.

Hilton, F., Armante, R., August, T., Barnet, C., Bouchard, A., Camy-Peyret, C., Capelle, V., Clarisse, L., Clerbaux, C., Coheur, P.-F., Collard, A., Crevoisier, C., Dufour, G., Edwards, D., Faijan, F., Fourrié, N., Gambacorta, A., Goldberg, M., Guidard, V., Hurtmans, D., Illingworth, S., Jacquinet-Husson, N., Kerzenmacher, T., Klaes, D., Lavanant, L., Masiello, G., Matricardi, M., McNally, A., Newman, S., Pavelin, E., Payan, S., Péquignot, E., Peyridieu, S., Phulpin, T., Remedios, J., Schlüssel, P., Serio, C., Strow, L., Stubenrauch, C., Taylor, J., Tobin, D., Wolf, W., Zhou, D.: Hyperspectral Earth Observation from IASI: four years of accomplishments, *B. Am. Meteorol. Soc.*, 93, 347–370, doi:10.1175/BAMS-D-11-00027.1, 2012.

Hoelzemann, J. J., Schultz, M. G., Brasseur, G. P., Granier, C., and Simon, M.: Global Wildland fire Emission Model (GWEM): evaluating the use of global area burnt satellite data, *J. Geophys. Res.*, 109, D14S04, doi:10.1029/2003JD003666, 2004.

Hollaway, T., Levy II, H., Kasibhatla, P.: Global distribution of carbon monoxide, *J. Geophys. Res.*, 105, 12123–12147, 2000.

IPCC: Climate Change 2007: The Physical Science Basis. Contribution of Working Group I to the Fourth Assessment Report of the Intergovernmental Panel on Climate Change, edited by: Solomon, S., Qin, D., Manning, M., Chen, Z., Marquis, M., Averyt, K. B., Tignor, M., and Miller, H. L., Cambridge University Press, Cambridge, UK and New York, NY, USA, 2007.

Jain, A. K., Tao, Z., Yang, X., Gillepsie, C.: Estimates of global biomass burning emissions for reactive greenhouse gases (CO, NMHCs, and NO<sub>x</sub>) and CO<sub>2</sub>, *J. Geophys. Res.*, 111, D06304, doi:10.1029/2005JD006237, 2006.

# Signature of tropical fires in the diurnal cycle of tropospheric CO as seen from Metop-A/IASI

T. Thonat et al.

Title Page

Abstract

Introduction

Conclusions

References

Tables

Figures

◀

▶

◀

▶

Back

Close

Full Screen / Esc

Printer-friendly Version

Interactive Discussion

- Kasischke, E. S. and Bruhwiler, L. P.: Emissions of carbon dioxide, carbon monoxide, and methane from boreal forest fires in 1998, *J. Geophys. Res.*, 108, 8146, doi:10.1029/2001JD000461, 2003.
- Langenfelds, R. L., Francey, R. J., Pak, B. C., Steele, L. P., Llyod, J., Trudinger, C. M., and Allison, C. E.: Interannual growth rate variations of atmospheric CO<sub>2</sub> and its  $\delta^{13}\text{C}$ , H<sub>2</sub>, CH<sub>4</sub>, and CO between 1992 and 1999 linked to biomass burning, *Global Biogeochem. Cy.*, 16, 1048, doi:10.1029/2001GB001466, 2002.
- Lavoué, D., Lioussé, C., Cahier, H., Stocks, B. J., and Goldammer, J. G.: Modeling of carbonaceous particles emitted by boreal and temperate wildland fires at northern latitudes, *J. Geophys. Res.*, 105, 26871–26890, 2000.
- Lehsten, V., Tansey, K., Balzter, H., Thonicke, K., Spessa, A., Weber, U., Smith, B., and Ar-neth, A.: Estimating carbon emissions from African wildfires, *Biogeosciences*, 6, 349–360, doi:10.5194/bg-6-349-2009, 2009.
- Lobert, J. M. and Warnatz, J.: Emissions from the combustion process in vegetation, in: *Fire in the Environment: the Ecological, Atmospheric, and Climatic Importance of Vegetation Fires*, edited by: Crutzen, P. J. and Goldammer, J. G., Wiley, Chichester, 15–37, 1993.
- Mayaux, P., Bartholome, E. M. C., Eva, H. D., Van Custem, C., Cabral, A., Nonguierna, A., Diallo, O., Pretorius, C., Thompson, M., Cherlet, M., Pekel, J.-F., Defourny, P., Vasconcelos, M., Di Gregorio, A., Fritz, S., De Grandi, G., Elvidge, C., Vogt, P., and Belward, A. S.: A Land Cover Map of Africa, *Carte de l'Occupation du Sol de l'Afrique*, European Commission, JRC24914, 2003.
- McMillan, W. W., Barnet, C., Strow, L., Chahine, M. T., McCourt, M. L., Warner, J. X., Novelli, P. C., Korontzi, S., Maddy, E. S., and Datta, S.: Daily global maps of carbon monoxide from NASA's Atmospheric Infrared Sounder, *Geophys. Res. Lett.*, 32, L11801, doi:10.1029/2004GL021821, 2005.
- McMillan, W. W., Warner, J. X., McCourt Comer, M., Maddy, E., Chu, A., sparling, L., Eloranta, E., Hoff, R., Sachse, G., Barnet, C., Razenkov, I., and Wolf, W.: AIRS views transport from 12 to 22 July 2004 Alaskan/Canadian fires: correlation of AIRS CO and MODIS AOD with forward trajectories and comparison of AIRS CO retrievals with DC-8 in situ measurements during INTEx-A/ICARITT, *J. Geophys. Res.*, 113, D20301, doi:10.1029/2007JD009711, 2008.

- Pierangelo, C., Chédin, A., Heilliette, S., Jacquinet-Husson, N., and Armante, R.: Dust altitude and infrared optical depth from AIRS, *Atmos. Chem. Phys.*, 4, 1813–1822, doi:10.5194/acp-4-1813-2004, 2004.
- Pyne, S. J., Andrews, P. L., and Laven, R. D.: *Introduction to Wildland Fire*, 2nd edn., John Wiley, New York, 14–25, 1996.
- Rio, C., Hourdin, F., and Chédin, A.: Numerical simulation of tropospheric injection of biomass burning products by pyro-thermal plumes, *Atmos. Chem. Phys.*, 10, 3463–3478, doi:10.5194/acp-10-3463-2010, 2010.
- Roberts, G., Wooster, M. J., and Lagoudakis, E.: Annual and diurnal african biomass burning temporal dynamics, *Biogeosciences*, 6, 849–866, doi:10.5194/bg-6-849-2009, 2009.
- Roy, D. P., Boschetti, L., Justice, C. O., and Ju, J.: The collection 5 MODIS burnt area product – global evaluation by comparison with the MODIS active fire product, *Remote Sens. Environ.*, 112, 3690–3707, 2008.
- Spivakovsky, C. M., Yevich, R., Logan, J. A., Wofsy, S. C., McElroy, M. B., and Prather, M. J.: Tropospheric OH in a three-dimensional chemical tracer model: an assessment based on observations of CH<sub>3</sub>CCl<sub>3</sub>, *J. Geophys. Res.*, 95, 18441–18471, 1990.
- Scott, N. A. and Chédin, A.: A fast line-by-line method for atmospheric absorption computations: the Automatized Atmospheric Absorption Atlas, *J. Appl. Meteorol.*, 20, 802–812, 1981.
- Seiler, W. and Crutzen, P. J.: Estimates of gross and net fluxes of carbon between the biosphere from biomass burning, *Climatic Change*, 2, 207–247, 1980.
- Streets, D. G., Zhang, Q., Wang, L., He, K., Hao, J., Wu, Y., Tang, Y., and Carmichael, G. R.: Revisiting China's CO emissions after Transport and Chemical Evolution over the Pacific (TRACE-P) mission: synthesis of inventories, atmospheric modeling, and observations, *J. Geophys. Res.*, 111, D14306, doi:10.1029/2006JD007118, 2006.
- Thonat, T., Crevoisier, C., Scott, N. A., Chédin, A., Schuck, T., Armante, R., and Crépeau, L.: Retrieval of tropospheric CO column from hyperspectral infrared sounders – application to four years of Aqua/AIRS and MetOp-A/IASI, *Atmos. Meas. Tech.*, 5, 2413–2429, doi:10.5194/amt-5-2413-2012, 2012.
- Turquety, S., Logan, J. A., Jacob, D. J., Hudman, R. C., Leung, F. Y., Heald, C. L., Yantosca, R. M., Wu, S., Emmons, L. K., Edwards, D. P., and Sachse, G. W.: Inventory of boreal fire emissions for North America in 2004: importance of peat burning and pyroconvective injection, *J. Geophys. Res.*, 112, D12S03, doi:10.1029/2006JD007281, 2007.

# Signature of tropical fires in the diurnal cycle of tropospheric CO as seen from Metop-A/IASI

T. Thonat et al.

Title Page

Abstract

Introduction

Conclusions

References

Tables

Figures

◀

▶

◀

▶

Back

Close

Full Screen / Esc

Printer-friendly Version

Interactive Discussion





# Signature of tropical fires in the diurnal cycle of tropospheric CO as seen from Metop-A/IASI

T. Thonat et al.

Title Page

Abstract

Introduction

Conclusions

References

Tables

Figures

◀

▶

◀

▶

Back

Close

Full Screen / Esc

Printer-friendly Version

Interactive Discussion



- Turquety, S., Hurtmans, D., Hadji-Lazaro, J., Coheur, P.-F., Clerbaux, C., Josset, D., and Tsamalis, C.: Tracking the emission and transport of pollution from wildfires using the IASI CO retrievals: analysis of the summer 2007 Greek fires, *Atmos. Chem. Phys.*, 9, 4897–4913, doi:10.5194/acp-9-4897-2009, 2009.
- 5 van der Werf, G. R., Randerson, J. T., Giglio, L., Collatz, G. J., Kasibhatla, P. S., and Arelano Jr., A. F.: Interannual variability in global biomass burning emissions from 1997 to 2004, *Atmos. Chem. Phys.*, 6, 3423–3441, doi:10.5194/acp-6-3423-2006, 2006.
- van der Werf, G. R., Randerson, J. T., Giglio, L., Collatz, G. J., Mu, M., Kasibhatla, P. S., Morton, D. C., DeFries, R. S., Jin, Y., and van Leeuwen, T. T.: Global fire emissions and the contribution of deforestation, savanna, forest, agricultural, and peat fires (1997–2009), *Atmos. Chem. Phys.*, 10, 11707–11735, doi:10.5194/acp-10-11707-2010, 2010.
- 10 Ward, D. E., Hao, W. M., Susott, R. A., Babitt, R. E., Shea, R. W., Kauffman, J. B., and Justice, C. O.: Effect of fuel composition efficiency and emission factors for African savanna ecosystems, *J. Geophys. Res.*, 101, 23569–23576, 1996.
- 15 Yurganov, N. L., McMillan, W. W., Dzhola, A. V., Grechko, E. I., Jones, N. B., and van der Werf, G. R.: Global AIRS and MOPITT CO measurements: validation, comparison, and links to biomass burning variations and carbon cycle, *J. Geophys. Res.*, 113, D09301, doi:10.1029/2007JD009229, 2008.
- 20 Yurganov, L. N., Rakitin, V., Dzhola, A., August, T., Fokeeva, E., George, M., Gorchakov, G., Grechko, E., Hannon, S., Karpov, A., Ott, L., Semutnikova, E., Shumsky, R., and Strow, L.: Satellite- and ground-based CO total column observations over 2010 Russian fires: accuracy of top-down estimates based on thermal IR satellite data, *Atmos. Chem. Phys.*, 11, 7925–7942, doi:10.5194/acp-11-7925-2011, 2011.



**Signature of tropical fires in the diurnal cycle of tropospheric CO as seen from Metop-A/IASI**

T. Thonat et al.

Title Page

Abstract

Introduction

Conclusions

References

Tables

Figures

◀

▶

◀

▶

Back

Close

Full Screen / Esc

Printer-friendly Version

Interactive Discussion

**Table 1.** Limits in latitude and longitude of the studied areas in southern Africa, corresponding to Fig. 4.

Code	Latitude	Longitude
H1	0–6° S	8–28° E
H2	0–6° S	28–43° E
H3	6–10° S	10–28° E
H4	6–10° S	28–40° E
H5	10–14° S	10–28° E
H6	10–14° S	28–43° E
H7	14–25° S	10–20° E
H8	14–25° S	20–28° E
H9	14–25° S	28–40° E
H10	12–25° S	42–50° E

# Signature of tropical fires in the diurnal cycle of tropospheric CO as seen from Metop-A/IASI

T. Thonat et al.

**Table 2.** Limits in latitude and longitude of the studied areas in the tropics, corresponding to Fig. 6. Af, Am, Aus respectively stand for Africa, America, Australia. N, S, E, W, respectively stand for North, South, East, West, and t stands for total.

Code	Latitude	Longitude	Code	Latitude	Longitude
AfNW	0–15° N	20° W–20° E	AfSE	0–20° S	25–40° E
AfNE	0–15° N	30–45° E	AfSt	0–25° S	10–40° E
AfNEC	0–15° N	20–45° E	Aft	25° N–25° S	20° W–43° E
AfN	0–15° N	20° W–45° E	AmSE	0–25° S	60–35° W
AfNt	0–25° N	20° W–45° E	AmC	0–25° N	110–62° W
AfSW	0–20° S	10–25° E	Aus	12–25° S	110–160° E

Title Page

Abstract

Introduction

Conclusions

References

Tables

Figures

◀

▶

◀

▶

Back

Close

Full Screen / Esc

Printer-friendly Version

Interactive Discussion

# Signature of tropical fires in the diurnal cycle of tropospheric CO as seen from Metop-A/IASI

T. Thonat et al.

Title Page

Abstract

Introduction

Conclusions

References

Tables

Figures

◀

▶

◀

▶

Back

Close

Full Screen / Esc

Printer-friendly Version

Interactive Discussion

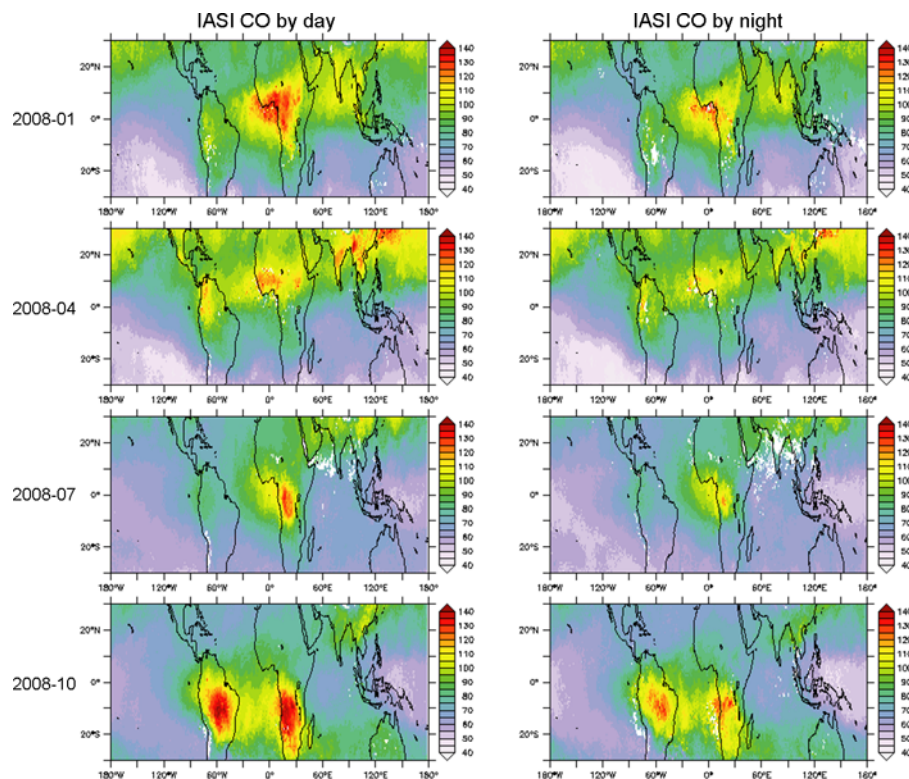


**Figure 1.** Monthly means of the integrated content of CO from IASI (ppbv), by day (9.30 a.m.) (left) and by night (9.30 p.m.) (right), in January, April, July and October 2008, in the tropics.

# Signature of tropical fires in the diurnal cycle of tropospheric CO as seen from Metop-A/IASI

T. Thonat et al.

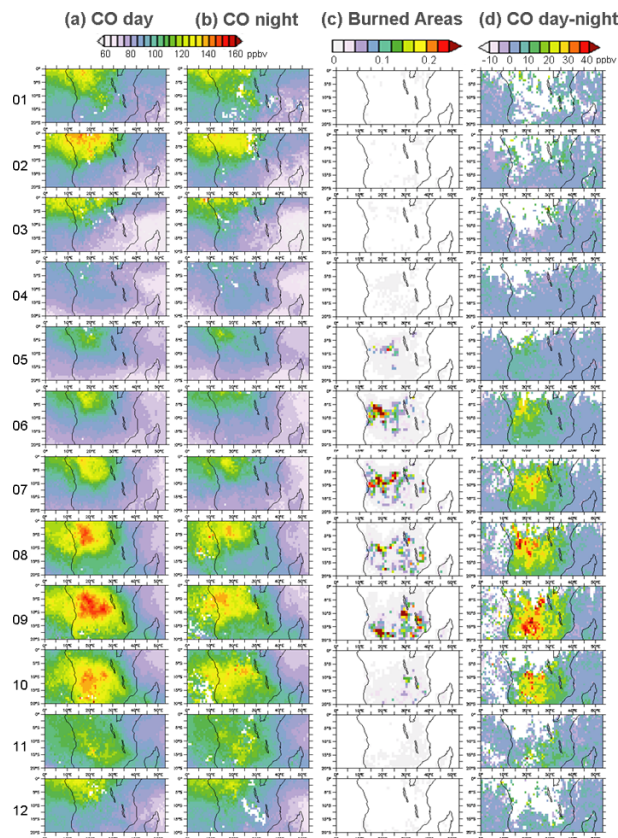


**Figure 2.** IASI CO and fires between January and December 2008, in southern Africa. **(a)** Monthly means of the integrated content of CO from IASI, by day (9.30 a.m.). **(b)** Same as **(a)**, by night (9.30 p.m.). **(c)** MODIS Burned Areas (Roy et al., 2008). **(d)** Monthly means of the day-night differences of the integrated content of CO from IASI.

[Title Page](#)
[Abstract](#)
[Introduction](#)
[Conclusions](#)
[References](#)
[Tables](#)
[Figures](#)
[◀](#)
[▶](#)
[◀](#)
[▶](#)
[Back](#)
[Close](#)
[Full Screen / Esc](#)
[Printer-friendly Version](#)
[Interactive Discussion](#)

# Signature of tropical fires in the diurnal cycle of tropospheric CO as seen from Metop-A/IASI

T. Thonat et al.

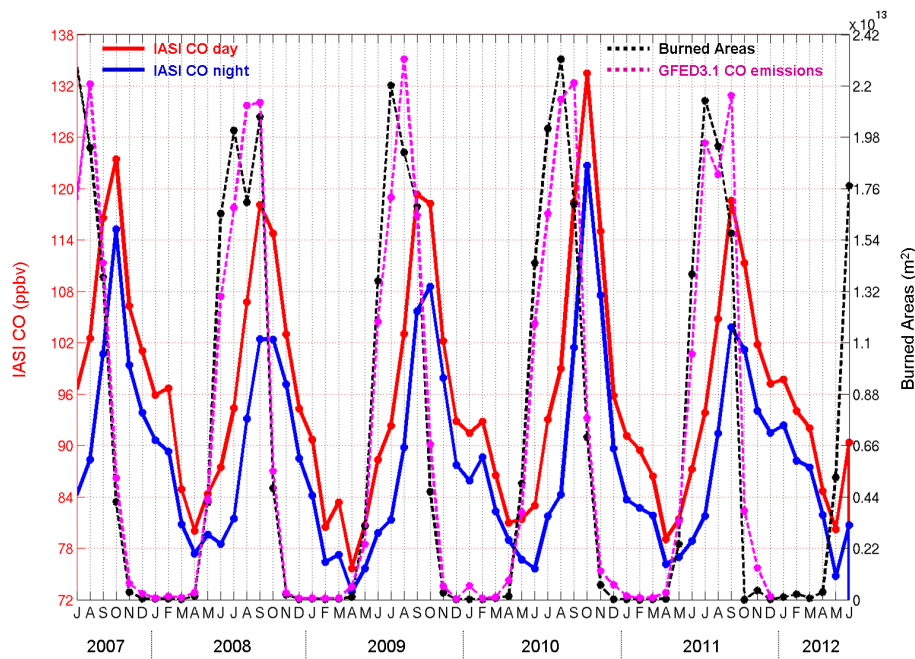


**Figure 3.** Evolution of the integrated content of CO from IASI on land and of fires between July 2007 and June 2012 in southern Africa (area comprised between 20° S and 0° in latitudes, and 0° and 53° E in longitudes.) Red: CO by day (9.30 a.m.). Blue: CO by night (9.30 p.m.). Black dashed: MODIS Burned Areas. Purple dashed: CO emissions from GFED3.1.

[Title Page](#)
[Abstract](#)
[Introduction](#)
[Conclusions](#)
[References](#)
[Tables](#)
[Figures](#)
[◀](#)
[▶](#)
[◀](#)
[▶](#)
[Back](#)
[Close](#)
[Full Screen / Esc](#)
[Printer-friendly Version](#)
[Interactive Discussion](#)

# Signature of tropical fires in the diurnal cycle of tropospheric CO as seen from Metop-A/IASI

T. Thonat et al.

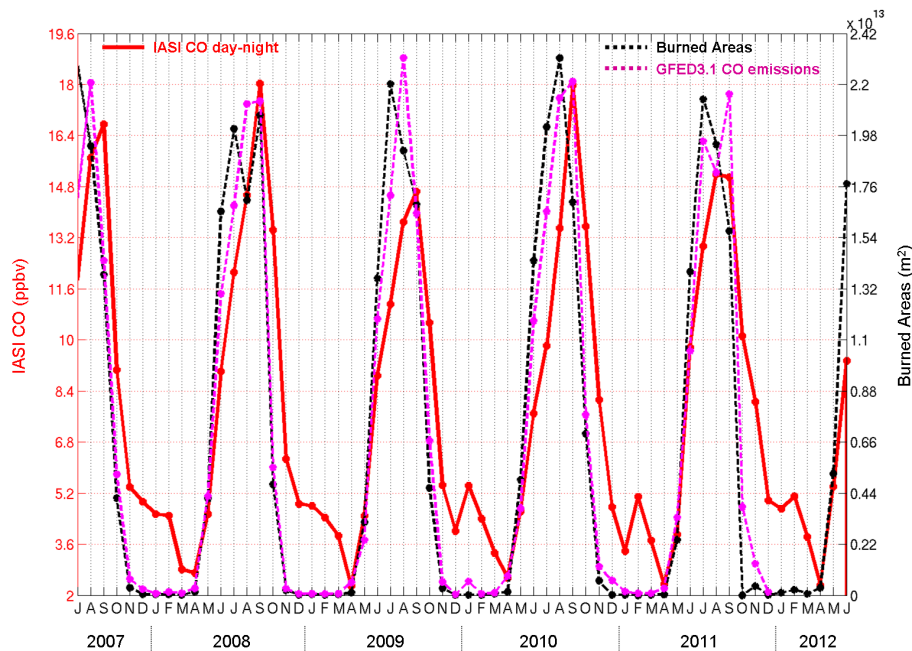


**Figure 4.** Evolution of the day-night difference of the integrated content of CO from IASI on land, and of fires, between July 2007 and June 2012 in southern Africa. Red: day-night CO. Black dashed: MODIS Burned Areas. Purple dashed: CO emissions from GFED3.1.

[Title Page](#)
[Abstract](#)
[Introduction](#)
[Conclusions](#)
[References](#)
[Tables](#)
[Figures](#)
[◀](#)
[▶](#)
[◀](#)
[▶](#)
[Back](#)
[Close](#)
[Full Screen / Esc](#)
[Printer-friendly Version](#)
[Interactive Discussion](#)

# Signature of tropical fires in the diurnal cycle of tropospheric CO as seen from Metop-A/IASI

T. Thonat et al.

Title Page

Abstract

Introduction

Conclusions

References

Tables

Figures

◀

▶

◀

▶

Back

Close

Full Screen / Esc

Printer-friendly Version

Interactive Discussion

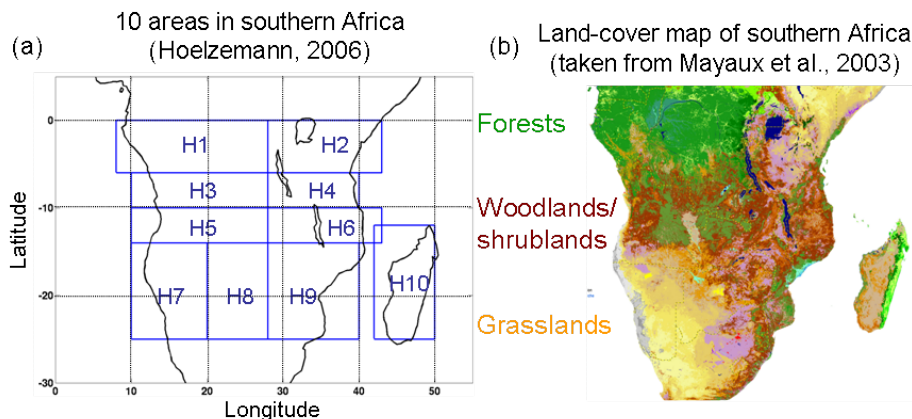


**Figure 5.** Definition of the studied areas in Africa. **(a)** Areas in Africa adapted from Hoelzemann, 2006. **(b)** Kinds of vegetation, adapted from Mayaux et al. (2003).



# Signature of tropical fires in the diurnal cycle of tropospheric CO as seen from Metop-A/IASI

T. Thonat et al.

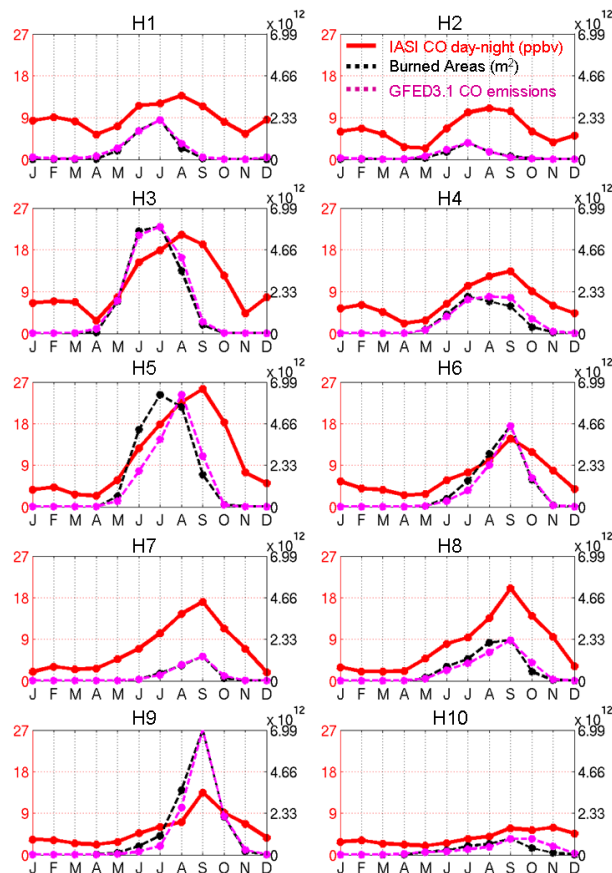


**Figure 6.** Evolution of the day-night difference of the integrated content of CO from IASI on land, and of fires, on average over 2008–2011 on different areas in southern Africa (see Fig. 5). Red: day-night CO. Black dashed: MODIS Burned Areas. Purple dashed: CO emissions from GFED3.1.

Title Page

Abstract

Introduction

Conclusions

References

Tables

Figures

◀

▶

◀

▶

Back

Close

Full Screen / Esc

Printer-friendly Version

Interactive Discussion



# Signature of tropical fires in the diurnal cycle of tropospheric CO as seen from Metop-A/IASI

T. Thonat et al.

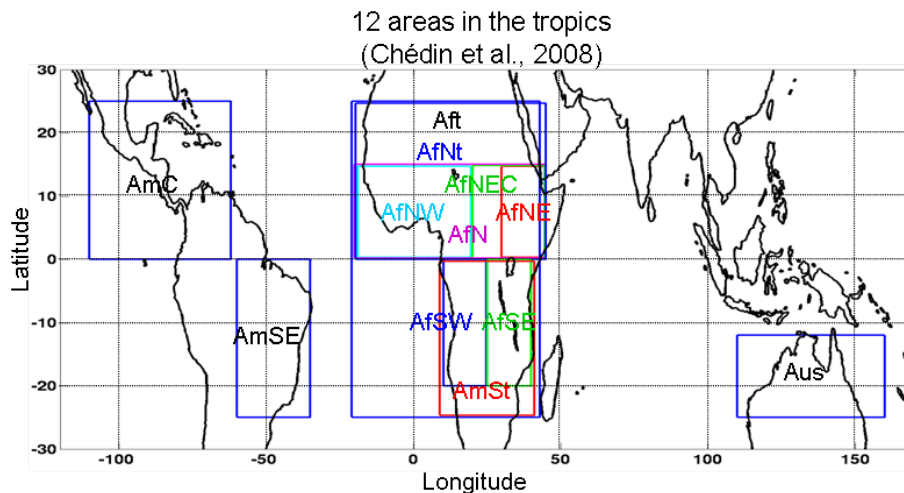


**Figure 7.** Definition of the studied areas in the tropics. Adapted from Chédin et al. (2008). Only lands are considered. Af, Am, Aus respectively stand for Africa, America, Australia. N, S, E, W, respectively stand for North, South, East, West, and t stands for total.

Title Page

Abstract

Introduction

Conclusions

References

Tables

Figures

◀

▶

◀

▶

Back

Close

Full Screen / Esc

Printer-friendly Version

Interactive Discussion

# Signature of tropical fires in the diurnal cycle of tropospheric CO as seen from Metop-A/IASI

T. Thonat et al.

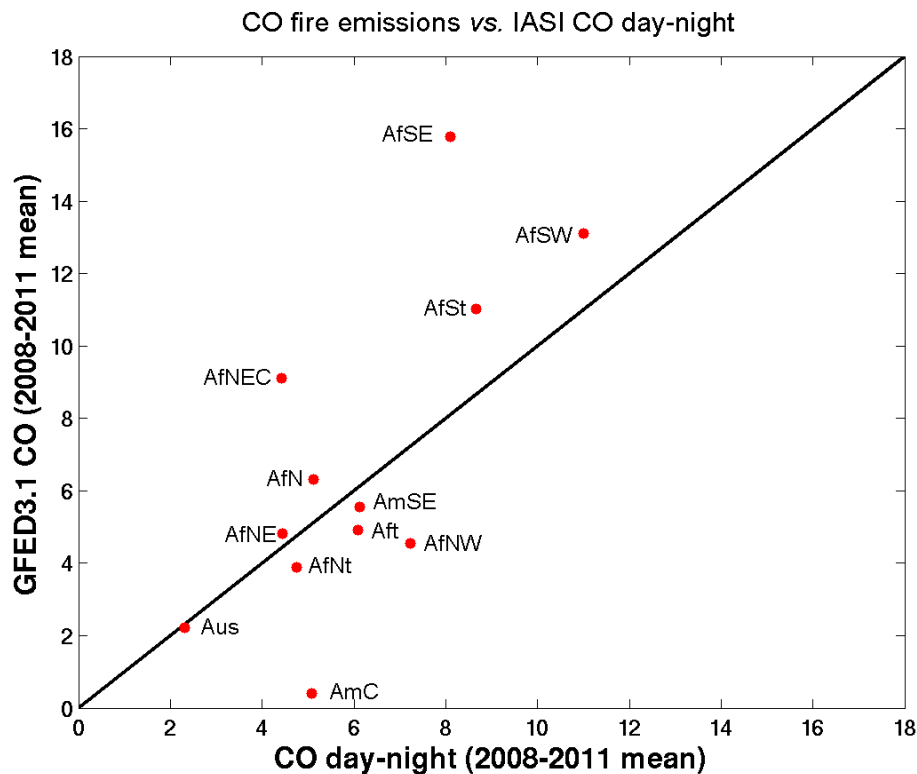


**Figure 8.** GFED3.1 emissions (in  $\text{g CO m}^{-2} \times 16$ ; see text Sect. 3.3) as a function of the day-night difference of the integrated content of CO from IASI (in ppbv) in different tropical areas (see Fig. 7). On average over 2008–2011.

[Title Page](#)
[Abstract](#)
[Introduction](#)
[Conclusions](#)
[References](#)
[Tables](#)
[Figures](#)
[◀](#)
[▶](#)
[◀](#)
[▶](#)
[Back](#)
[Close](#)
[Full Screen / Esc](#)
[Printer-friendly Version](#)
[Interactive Discussion](#)

# Signature of tropical fires in the diurnal cycle of tropospheric CO as seen from Metop-A/IASI

T. Thonat et al.

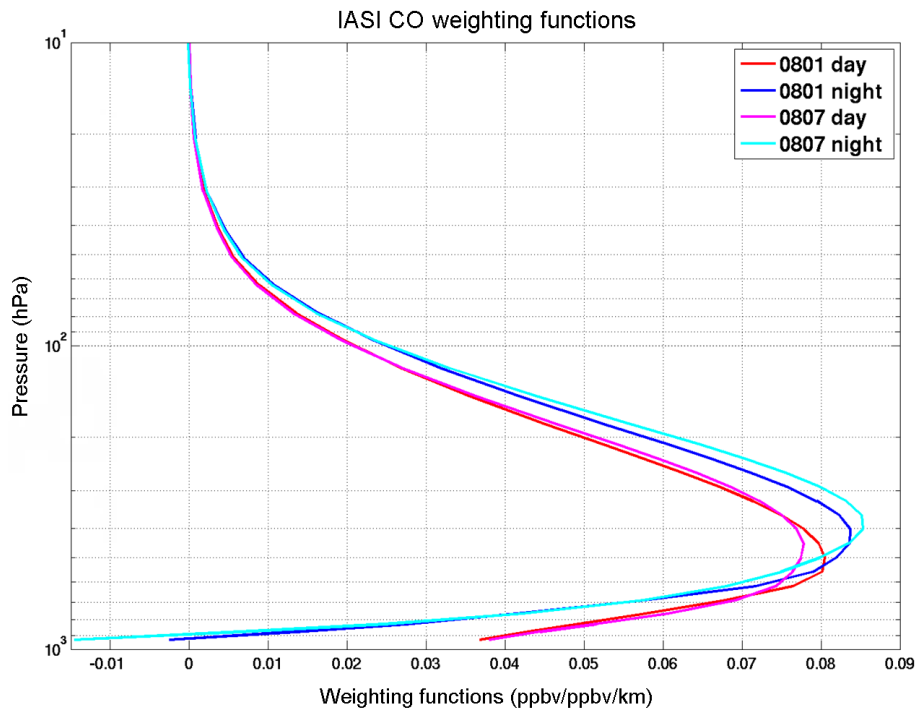


**Figure 9.** IASI CO weighting functions ( $\text{ppbv ppbv}^{-1} \text{ km}^{-1}$ ), averaged over southern Africa, on land. Red: January by day (09:30). Blue: January by night (21:30). Magenta: July by day. Cyan: July by night.

[Title Page](#)[Abstract](#)[Introduction](#)[Conclusions](#)[References](#)[Tables](#)[Figures](#)[◀](#)[▶](#)[◀](#)[▶](#)[Back](#)[Close](#)[Full Screen / Esc](#)[Printer-friendly Version](#)[Interactive Discussion](#)

# Signature of tropical fires in the diurnal cycle of tropospheric CO as seen from Metop-A/IASI

T. Thonat et al.

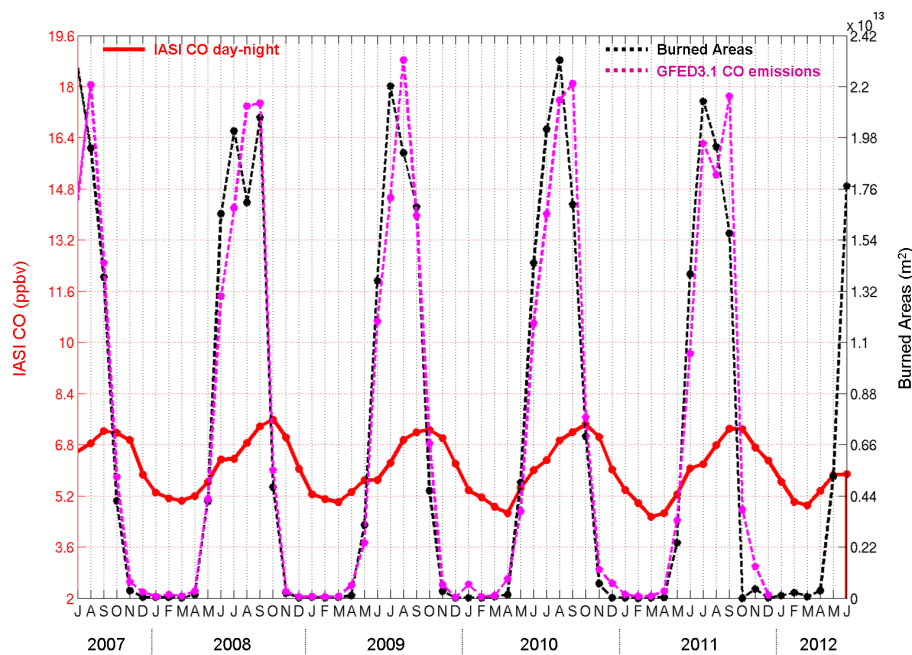


**Figure 10.** Evolution of the day-night difference of the integrated content  $qCO^{4A}$  (see text Sect. 4.1) on land, and of fires, between July 2007 and June 2012 in southern Africa. Red: day-night CO. Black dashed: MODIS Burned Areas. Purple dashed: CO emissions from GFED3.1.

[Title Page](#)
[Abstract](#)
[Introduction](#)
[Conclusions](#)
[References](#)
[Tables](#)
[Figures](#)
[◀](#)
[▶](#)
[◀](#)
[▶](#)
[Back](#)
[Close](#)
[Full Screen / Esc](#)
[Printer-friendly Version](#)
[Interactive Discussion](#)

# Signature of tropical fires in the diurnal cycle of tropospheric CO as seen from Metop-A/IASI

T. Thonat et al.

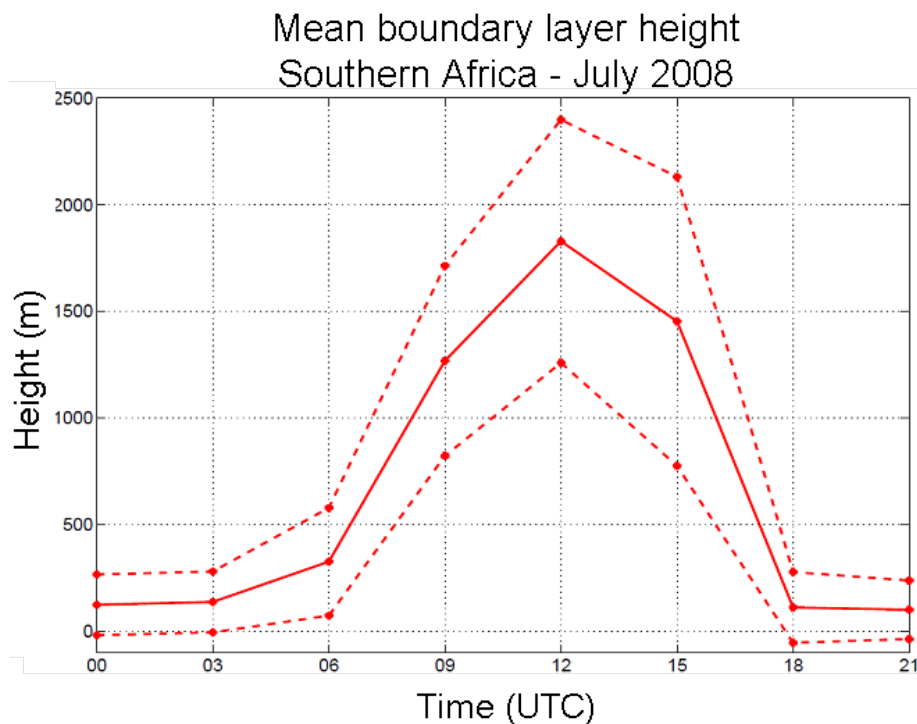


**Figure 11.** Mean boundary layer height (solid line) in southern Africa and SD (dashed lines). Plotted from the ECMWF forecasts, which have a 3 h time step and a  $0.75^\circ \times 0.75^\circ$  spatial resolution.

[Title Page](#)
[Abstract](#)
[Introduction](#)
[Conclusions](#)
[References](#)
[Tables](#)
[Figures](#)
[◀](#)
[▶](#)
[◀](#)
[▶](#)
[Back](#)
[Close](#)
[Full Screen / Esc](#)
[Printer-friendly Version](#)
[Interactive Discussion](#)